JOURNAL OF MATERIALS SCIENCE 37 (2002) 3533–3540

Modelling of kinetics and dilatometric behaviour of austenite formation in a low-carbon steel with a ferrite plus pearlite initial microstructure

F. G. CABALLERO, C. CAPDEVILA, C. GARCÍA DE ANDRÉS
Department of Physical Metallurgy, Centro Nacional de Investigaciones Metalúrgicas (CENIM), Consejo Superior de Investigaciones Científicas (CSIC), Avda. Gregorio del Amo, 8. 28040 Madrid, Spain
E-mail: cgda@cenim.csic.es

The compiled knowledge in literature regarding the isothermal formation of austenite from different initial microstructures (pure and mixed microstructures), has been used in this work to develop a model for non-isothermal austenite formation in low-carbon steels ($C < 0.2$ wt%) with a mixed initial microstructure consisting of ferrite and pearlite. Likewise, calculations of relative change in length have been made as a function of temperature, and the differences between theoretical and experimental results have been analysed in 0.1C–0.5Mn low-carbon low-manganese steel. Experimental kinetic transformation, critical temperatures as well as the magnitude of the overall contraction due to austenite formation are in good agreement with calculations.

1. Introduction

Most commercial processes rely on heat treatments which cause the steel to revert to the austenitic condition. This includes the processes involved in the manufacture of wrought steels and in the fabrication of steel components by welding. The formation of austenite is an inevitable occurrence during the heat treatment of steels. The phenomenon of austenitisation has been studied in the past but the work has tended to be disconnected and at a qualitative level. The initial condition of the austenite determines the development of the final microstructure and mechanical properties, so it is useful to model the transformation into austenite. In this sense, a quantitative theory dealing with the nucleation and growth of austenite from a variety of initial microstructural conditions is vital [1].

Early work on austenitisation prior to 1940 was summarised in a paper by Roberts and Mehl [2], which also reported a study of austenite formation from ferrite/pearlite and ferrite/"spheroidite" aggregates establishing the nucleation and growth character of the transformation. Subsequent work indicated the importance of cementite precipitates in ferrite in aiding nucleation of austenite [3, 4], and considered austenite growth controlled by cementite dissolution [3, 5–7]. These investigations give an indication of the complexity of the problem since the austenite nucleates and grows in a microstructure consisting of two phases which have different degrees of stability.

In the eighties, the development of dual-phase steels by partial austenitisation revived the interest for the heating part of the heat treatment cycle. Dual-phase steels, widely used in the automobile industry, are characterised by a superior combination of mechanical properties. These steels are produced by annealing low-carbon steels in the intercritical temperature range with the aim of obtaining ferrite-austenite mixtures, and subsequent quenching to transform the austenite phase into martensite [8–10]. They have demonstrated that a ferrite-martensite microstructure promotes continuous yielding with a rapid rate of work hardening and improved elongation in comparison to a ferrite-pearlite microstructure [11]. Speich *et al*. [12] categorised the intercritical austenitisation in low-carbon steels with a ferrite-pearlite starting microstructure into three stages: (a) pearlite dissolution and growth of austenite into pearlite at a rate controlled primarily by carbon diffusion in the austenite; the growth rate of the austenite in this stage is expected to be rapid [12–15]; (b) slower growth of austenite into ferrite; and (c) slow equilibration in chemical composition of ferrite and austenite. García and DeArdo [11] pointed out that before complete dissolution of pearlite, the lamellar cementite particles spherodise and the carbon from the cementite particles diffuses towards the growing austenite. These authors all emphasised the importance of the microstructure that exists before intercritical annealing.

Little information is available about the austenite formation in steels subjected to continuous heating [16]. Recent work has quantitatively modelled the transformation of an ambient temperature steel microstructure into austenite during continuous heating [17, 18]. In these investigations, the Avrami equation, generally used to model transformations under isothermal conditions, was successfully applied to the pearlite-to-austenite transformation during continuous heating in a

eutectoid steel with a fully pearlitic initial microstructure. Lately, some researchers have adopted a different approach to the problem using artificial neural network [19, 20], which helped to identify the fact that a neglect of the starting microstructure can lead to major errors in the transformation temperatures, sometimes by more than 100°C.

All the theoretical knowledge [3, 6, 12, 15, 21–24] regarding the isothermal formation of austenite from different initial microstructures (pure and mixed microstructures), will be used in this work to develop a model for the non-isothermal austenite formation in low-carbon steels with a mixed initial microstructure consisting of ferrite and pearlite.

Since dilatometric analysis is a technique very often employed to study phase transformations in steels, calculations of relative change in length have been made as a function of temperature, and the differences between theoretical and experimental results have been analysed in 0.1C–0.5Mn low-carbon low-manganese steel. Moreover, high-resolution dilatometry and metallographic analysis have been used to study the dissolution of pearlite during continuous heating in the same steel. A clear differentiation between pearlite dissolution process and $\alpha \rightarrow \gamma$ transformation has been found. The influence of the pearlite morphology on dissolution process has been also studied in this work.

2. Materials and experimental procedure

The chemical composition of the steel studied in this research work is presented in Table I. Semi rolled slabs 36 mm thick were soaked at 1523 K for 15 min., hot rolled to 6 mm in several passes, and finally air cooled to room temperature. The as-rolled microstructure of the steel is formed approximately by 90% ferrite and 10% pearlite (Fig. 1a).

Specimens were polished in the usual way and finished on 0.5 μm diamond paste for metallographic examination. Two types of etching solution were used: Nital-2pct to reveal the ferrite-pearlite microstructure by light optical microscopy and solution of picric acid in isopropyl alcohol with several drops of Vilella's reagent to disclose the pearlite morphology on a JEOL JXA 840 scanning electron microscope. Fig. 1b shows a scanning micrograph of the morphology of pearlite considered in this study.

Two parameters, the mean true interlamellar spacing, σ_o, and the area per unit volume of the pearlite colonies interface, S_v^{PP}, characterise the morphology of pearlite [15]. The values of σ_o were derived from electron micrographs according to Underwood's intersection procedure. Underwood [25] recommends determining the mean random spacing, σ_r, first to estimate the mean true spacing, σ_o. For this purpose, a circular test grid of diameter d_c is superimposed on an electron micrograph.

TABLE I Chemical composition of low-carbon low-manganese steel (mass %)

C	Mn	Si	Cr	Ni
0.11	0.50	0.03	0.01	0.02

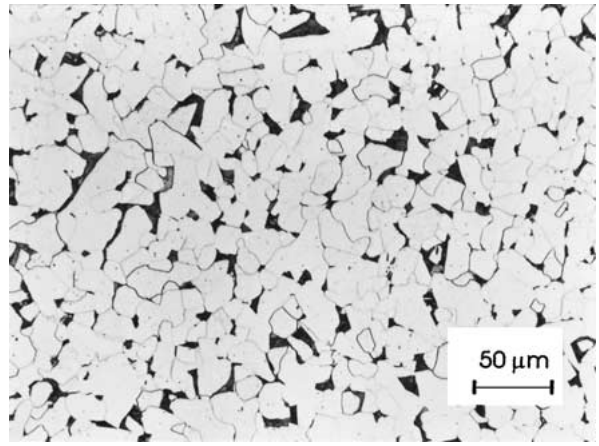

(a)

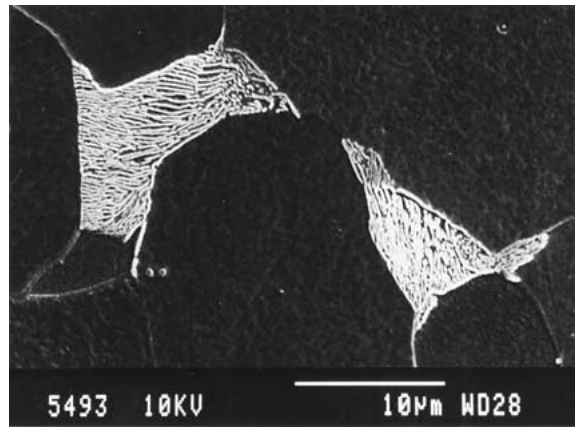

(b)

Figure 1 Initial microstructure of the steel considered in this study: (a) Optical micrograph; (b) Scanning electron micrograph.

The number n of intersections of lamellae of carbide with the test grid is counted. This procedure is repeated on a number of fields chosen randomly. Then, the mean random spacing, σ_r, is calculated from:

$$\sigma_r = \frac{\pi d_c}{nM} \tag{1}$$

where M is the magnification of the micrograph.

Saltykov [26] has shown that, for pearlite with a constant spacing within each colony, the mean true spacing, σ_o, is related to the mean random spacing, σ_r, by:

$$\sigma_o = \frac{\sigma_r}{2} \tag{2}$$

The values of S_v^{PP} were measured on scanning micrographs by counting the number of intersections, n', of the pearlite colony boundaries with a circular test grid of diameter d_c' as reported by Roosz *et al.* [15]. Then, the area per unit volume of the pearlite colonies interface is:

$$S_v^{PP} = \frac{2n'M}{\pi d_c'} \tag{3}$$

Approximating the pearlite colony by a truncated octahedron, the edge length of the pearlite colonies, a^P, is

TABLE II Morphological characterisation of initial microstructure

V_{P_o}	$\sigma_o \times 10^{-3}$ (mm)	S_v^{PP} (mm^{-1})	$a^P \times 10^{-3}$ (mm)
0.11 ± 0.04	0.15 ± 0.02	959 ± 154	2.5 ± 0.5

calculated from the area per unit volume S_v^{PP} with the following expression [27]:

$$S_v^{PP} = \frac{6(1+2\sqrt{3})(a^P)^2}{8\sqrt{2}(a^P)^3} = \frac{3(1+2\sqrt{3})}{4\sqrt{2}a^P} \quad (4)$$

Data for σ_o, S_v^{PP} and a^P are listed in Table II.

To validate the austenitisation model and the calculated dilatation curve, an Adamel Lhomargy DT1000 high-resolution dilatometer was used. For this purpose, dilatometric specimens 2 mm thick and 12 mm long were heated at a constant rate of 0.05 Ks^{-1} in a vacuum of 1 Pa. The dimensional variations in the specimen are transmitted via an amorphous silica pushrod. These variations are measured by a linear variable differential transformer (LVDT) in a gas-tight enclosure enabling to test under vacuum or in an inert atmosphere. The DT1000 dilatometer is equipped with a radiation furnace for heating. The energy radiated by two tungsten filament lamps is focused on the dilatometric specimen by means of a bi-elliptical reflector. The temperature is measured with a 0.1 mm diameter Chromel-Alumel (type K) thermocouple welded to the specimen. Cooling is carried out by blowing a jet of helium gas directly onto the specimen surface. The helium flow rate during cooling is controlled by a proportional servovalve. The high efficiency of heat transmission and the very low thermal inertia of the system ensure that the heating and cooling rates ranging from 0.003 Ks^{-1} to 200 Ks^{-1} remain constant.

3. Results and discussion

3.1. Modelling of kinetics of non-isothermal austenite formation in a steel with a ferrite plus pearlite initial microstructure

In the austenitisation of microstructures composed of ferrite and pearlite, two different transformations are involved: pearlite dissolution and ferrite-to-austenite transformation. Both transformations take place by nucleation and growth processes.

3.1.1. Modelling of kinetics of dissolution of pearlite

Nucleation and growth processes under isothermal condition can be described in general using the Avrami's equation [28]:

$$x = 1 - \exp(-Kt^n) \quad (5)$$

where x represents the formed austenite volume fraction in the austenitisation of a fully pearlitic microstructure, K is a constant for a given temperature, t is the time and n is a constant characterising the kinetics. Roosz *et al.* [15] obtained a value of $n = 4$ from their measured data during intercritical annealing of a eutectoid plain carbon steel. According to Christian [29], with a spherical configuration, a value of $n = 4$ means that the nucleation rate ($\dot{N}$) and the growth rate (G) are constant in time. This gives a transformed volume fraction of:

$$x = 1 - \exp\left(-\frac{\pi}{3}\dot{N}G^3t^4\right) \quad (6)$$

Roosz *et al.* [15] proposed the following temperature and structure dependence of nucleation and growth rates of austenite inside pearlite as a function of the reciprocal value of overheating ($\Delta T = T - Ac_1$),

$$\dot{N} = f_N \exp\left(\frac{-Q_N}{k\Delta T}\right) \quad (7)$$

$$G = f_G \exp\left(\frac{-Q_G}{k\Delta T}\right) \quad (8)$$

where Q_N and Q_G are the activation energies of nucleation and growth [15], respectively, k is Boltzmann's constant, and f_N and f_G are the functions representing the influence of the structure on the nucleation and growth rates, respectively.

The morphological function f_N in Equation 7 was found in previous authors' work [18] to have the following general form:

$$f_N = K_N \frac{(a^P)^n}{\sigma_o^m}(N_C)^i \quad (9)$$

where a^P is the edge length of the pearlite colony, σ_o is the interlamellar spacing, N_C is the number of nucleation sites (points of intersection of cementite with the edges of the pearlite colony [3, 21]) per unit volume $\left(N_C \approx 1/(a^P)^2\sigma_o\right)$ and K_N, n, m and i are empirical parameters. In this previous authors' work [18], a model that describes pearlite-to-austenite transformation during continuous heating in a eutectoid steel was developed and the influence of morphological parameters on the austenite formation kinetics was experimentally studied and considered in the modelling.

Moreover, if the growth of austenite is considered to be controlled by interface diffusion of substitutional elements [15], the function f_G in Equation 8 representing the structure dependence on the growth rate can be expressed as follows:

$$f_G = K_G \frac{1}{\sigma_o^2} \quad (10)$$

where K_G is a empirical constant [18].

The difficulties in treating non-isothermal reactions are meanly due to the independent variations of growth and nucleation rates with temperature. The problem is only undertaken when the rate of transformation depends exclusively on the state of the assembly and not

on the thermal path by which the state is reached [29]. Reactions of this type are called isokinetic. Avrami defined an isokinetic reaction by the condition that the nucleation and growth rates are proportional to each other (i.e., they have the same temperature variation). This leads to the concept of additivity and Scheil's rule [30].

Since Avrami's condition for an isokinetic reaction is not satisfied for the current experimental study, a general equation to describe the non-isothermal overall pearlite-to-austenite transformation in a pearlitic steel was derived integrating the Avrami's equation over the whole temperature range where the transformation takes place [17]. In this sense, logarithms were taken in Equation 6 and then it was differentiated,

$$d\left(\ln\frac{1}{1-x}\right)=\frac{\mathrm{d}x}{1-x}=\frac{4\pi}{3}\dot{N}G^3t^3\mathrm{d}t \qquad (11)$$

If we consider a constant rate for the heating condition ($\dot{T}$), time can be expressed as follows:

$$\mathrm{d}t=\frac{\mathrm{d}T}{\dot{T}} \qquad t=\frac{\Delta T}{\dot{T}} \qquad (12)$$

and substituting into Equation 11 and integrating in $[0, x]$ and $[Ac_1, T]$ intervals on the left and on the right sides, respectively, it can be concluded that:

$$x=1-\exp\left(-\int_{Ac_1}^{T}\frac{4\pi}{3(\dot{T})^4}\dot{N}G^3\Delta T^3\mathrm{d}T\right) \qquad (13)$$

where x represents the formed austenite volume fraction in the austenitisation of a fully pearlitic microstructure and, $\dot{N}$ and G are given by Equations 7 and 8. Thus, the austenite volume fraction obtained from pearlite dissolution V_γ^P during continuous heating of a ferrite plus pearlite initial microstructure is expressed as follows:

$$V_\gamma^P=V_{P_o}\left\{1-\exp\left(-\int_{Ac_1}^{T}\frac{4\pi}{3(\dot{T})^4}\dot{N}G^3\Delta T^3\mathrm{d}T\right)\right\} \qquad (14)$$

where V_{P_o} is the volume fraction of pearlite present in the initial microstructure. The eutectoid temperature Ac_1 of the steel was obtained using Andrews' formula [31].

3.1.2. Modelling of kinetics of ferrite-to-austenite transformation after dissolution of pearlite

Datta *et al*. [23] carried out a quantitative microstructural analysis of the austenitisation kinetics of pearlite and ferrite aggregates at different intercritical annealing temperatures in a low-carbon steel containing 0.15 wt% C. At all the tested temperatures, pearlite-to-austenite transformation was complete in less than one second and the kinetics of the ferrite-to-austenite transformation at higher temperatures ($T \geq 1143$ K) [23] were found to be different from those tested at lower temperatures ($T < 1143$ K) [23]. In this sense, the time (t) dependence of the volume fraction of austenite V_γ at different temperatures was described by the following linear relationships:

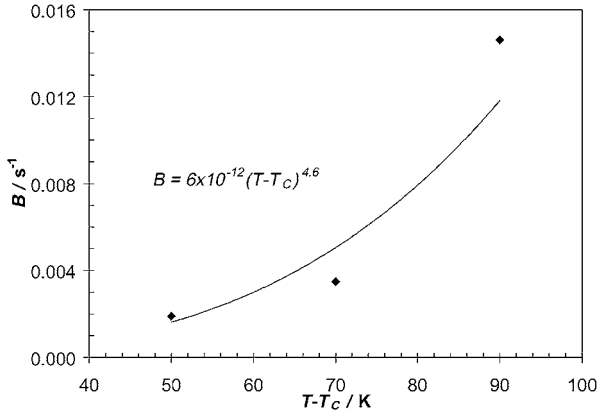

Figure 2 Temperature dependence of the kinetics parameter B from Datta *et al*. [23] experimental results. T_C is the temperature at which ferrite-to-austenite transformation starts during the continuous heating of a ferrite plus pearlite initial microstructure.

$$\frac{V_\gamma}{1-V_\gamma}=\frac{V_\gamma^\alpha+V_{P_o}}{V_{\alpha_o}-V_\gamma^\alpha}=A+Bt \quad \text{for} \quad T<1143\,\mathrm{K} \qquad (15)$$

$$\frac{V_\gamma}{1-V_\gamma}=\frac{V_\gamma^\alpha+V_{P_o}}{V_{\alpha_o}-V_\gamma^\alpha}=A'+B't^2 \quad \text{for} \quad T\geq 1143\,\mathrm{K} \qquad (16)$$

where V_γ^α is the austenite volume fraction formed from ferrite after complete pearlite-to-austenite transformation and, V_{P_o} and V_{α_o} are the volume fractions of pearlite and ferrite, respectively, present in the initial microstructure. The parameters A, A' and B' are insensitive to temperature ($A \approx 0.20$, $A' = 0.25$ and $B' = 1.2 \times 10^{-3}$ s^{-2}) [23], whereas B changes significantly with temperature. Fig. 2 shows temperature dependence of the kinetic parameter B from Datta *et al*. [23] experimental results, being T_C the starting temperature of ferrite-to-austenite transformation and $T - T_C$ the overheating for this transformation.

With the aim of adapting Equations 15 and 16 to non-isothermal conditions, we have differentiated both equations.

$$\frac{\mathrm{d}V_\gamma^\alpha}{\left(V_{\alpha_o}-V_\gamma^\alpha\right)^2}=B\mathrm{d}t \quad \text{for} \quad T_C<T<T_D \qquad (17)$$

$$\frac{\mathrm{d}V_\gamma^\alpha}{\left(V_{\alpha_o}-V_\gamma^\alpha\right)^2}=2B't\,\mathrm{d}t \quad \text{for} \quad T\geq T_D \qquad (18)$$

where T_C is the previously cited temperature and T_D the temperature at which the kinetics of ferrite-to-austenite transformation changes under non-isothermal conditions. It should be noticed that these critical temperatures do not have to correspond with those from Datta *et al*. study since their work was carried out under isothermal conditions.

Expressing time as $t=\frac{T-T_C}{\dot{T}}$, where $\dot{T}$ is the heating rate and integrating in $\left[0, V_\gamma^\alpha\right]$ and $[T_C, T]$ intervals

on the left and on the right sides of Equation 17, respectively, and in $\left[V_D^\alpha, V_\gamma^\alpha\right]$ and $[T_D, T]$ intervals on the left and on the right sides of Equation 18, respectively, it can be concluded that:

$$\int_0^{V_\gamma^\alpha} \frac{\mathrm{d}V_\gamma^\alpha}{\left(V_{\alpha_o} - V_\gamma^\alpha\right)^2} = \int_{T_C}^{T} \frac{6 \times 10^{-12}(T - T_C)^{4.6}}{\dot{T}}\,\mathrm{d}T \quad \text{for} \quad T_C < T < T_D \quad (19)$$

$$\int_{V_D^\alpha}^{V_\gamma^\alpha} \frac{\mathrm{d}V_\gamma^\alpha}{\left(V_{\alpha_o} - V_\gamma^\alpha\right)^2} = \int_{T_D}^{T} \frac{2.4 \times 10^{-3}(T - T_C)}{(\dot{T})^2}\,\mathrm{d}T \quad \text{for} \quad T \geq T_D \quad (20)$$

where V_D^α is the austenite volume fraction formed from ferrite at T_D temperature.

Thus, the volume fraction of austenite formed from ferrite during continuous heating at a given temperature is expressed as follows:

$$V_\gamma^\alpha = V_{\alpha_o}\left[1 - \frac{5.6\dot{T}}{6 \times 10^{-12}\, V_{\alpha_o}(T - T_C)^{5.6} + 5.6\dot{T}}\right] \quad \text{for} \quad T_C < T < T_D \quad (21)$$

$$V_\gamma^\alpha = V_{\alpha_o} - \frac{\left(V_{\alpha_o} - V_D^\alpha\right)(\dot{T})^2}{(\dot{T})^2 + 1.2 \times 10^{-3}\left(V_{\alpha_o} - V_D^\alpha\right)\left[(T - T_C)^2 - (T_D - T_C)^2\right]} \quad \text{for} \quad T \geq T_D \quad (22)$$

T_C and T_D temperatures were determined experimentally for this steel by means of dilatometric analysis. The possibility to be able to discriminate the pearlite dissolution process and the ferrite-to-austenite transformation by means of high resolution dilatometry permitted the determination of T_C. As Datta *et al.* [23] found under isothermal conditions, a change on ferrite-to-austenite growth kinetics has been also detected in this work by the above mentioned technique enabling T_D experimental determination. Fig. 3 shows the experimental dilatometric curve for a heating rate of 0.05 Ks^{-1}. This curve is the average of four identical dilatometric tests. T_C and T_D temperatures are displayed on the curve in accordance with their definition above. Ac_1 and Ac_3 critical temperatures represent the starting and finishing temperatures of the austenitisation process.

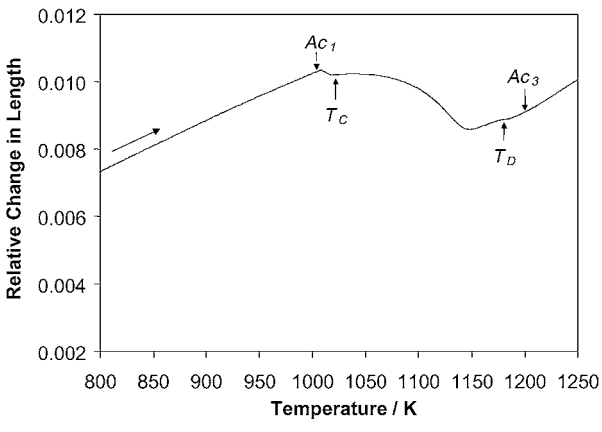

Figure 3 Experimental dilatation curve, average of four identical dilatometric tests, of the studied steel for a heating rate of 0.05 Ks^{-1}.

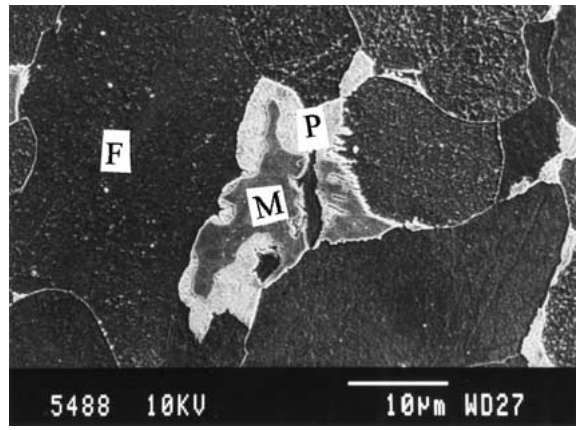

Figure 4 Scanning electron micrograph of the microstructure obtained by interrupted heating by quenching at 10 K after Ac_1 temperature. P is pearlite, M is martensite and F is ferrite.

Normally, no differentiation between pearlite dissolution process and $\alpha \rightarrow \gamma$ transformation is detected in the heating dilatometric curve of a ferrite plus pearlite microstructure. However, the experimental curve in Fig. 3 shows an unusual well formed contraction which could be associated to the pearlite dissolution. To confirm that this anomaly effectively corresponds to the pearlite-to-austenite transformation, a specimen was heated up to 10 K above the temperature of the dilatometric peak, which corresponds to Ac_1 temperature, at a heating rate of 0.05 Ks^{-1}, and immediately quenched at a cooling rate of 500 Ks^{-1}, approximately. Micrograph in Fig. 4 show the microstructure obtained in the interrupted heating test at that temperature (1018 K). It is clear from Fig. 4 that the dissolution of pearlite took place during heating at temperatures higher than the dilatometric peak temperature. In this sense, the previously defined Ac_1 and T_C are the starting and finishing temperatures, respectively, of this anomaly. These temperatures have been determined from dilatometric analysis and also verified by metallography obtaining $Ac_1 = 1008$ K and $T_C = 1023$ K.

Likewise, the small contraction after the relative change in length reached to a minimum corresponds to the formation of austenite from some grains of ferrite that remains untransformed in the microstructure. This would explain the change in the linear thermal expansion as those residual ferrite grains transform almost instantaneously at T_D temperature due to the change in ferrite-to-austenite transformation kinetics.

Fig. 5 represents the calculated volume fraction of the different microconstituents as a function of temperature. From this diagram it can be seen that the eutectoid transformation (pearlite curve) proceeds within a narrow temperature range (between Ac_1 and T_C temperatures). This transformation needs about 15 K to reach completion in this steel for a heating rate of 0.05 Ks^{-1}. The austenite curve clearly reproduces the two different growth kinetics that occur during

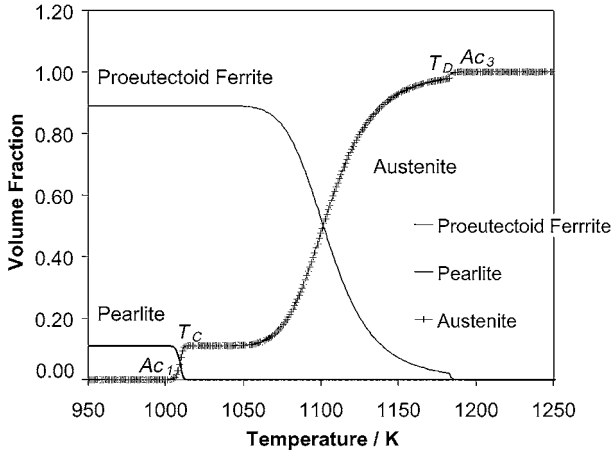

Figure 5 Calculated volume fraction of the different phases present in the microstructure as a function of temperature.

ferrite-to-austenite transformation. At temperatures lower than T_D, the transformation reproduces an usual kinetic behaviour, whereas at temperatures higher than T_D, the kinetics suddenly increases promoting the completion of austenitisation process only a few degrees after.

3.2. Modelling of dilatometric behaviour of non-isothermal austenite formation in a steel with a ferrite plus pearlite initial microstructure

Assuming that the sample expands isotropically, the change of the sample length ΔL referred to the initial length L_o at room temperature is related to volume change ΔV and initial volume V_o at room temperature for small changes as follows:

$$\frac{\Delta L}{L_o} = \frac{V - V_o}{3V_o} \tag{23}$$

Therefore, $\frac{\Delta L}{L_o}$ can be calculated from the volumes of the unit cells and the volume fractions of the different phases present in the microstructure at every temperature during continuous heating:

$$\frac{\Delta L}{L_o} = \frac{1}{3}\left[\frac{\left(2V_\alpha a_\alpha^3 + \frac{1}{3}V_\theta a_\theta b_\theta c_\theta + V_\gamma a_\gamma^3\right) - \left(2V_{\alpha_o} a_{\alpha_o}^3 + \frac{1}{3}V_{\theta_o} a_{\theta_o} b_{\theta_o} c_{\theta_o}\right)}{\left(2V_{\alpha_o} a_{\alpha_o}^3 + \frac{1}{3}V_{\theta_o} a_{\theta_o} b_{\theta_o} c_{\theta_o}\right)}\right] \tag{24}$$

with $V_{\theta_o} = 0.12V_{P_o}$ and $V_{\alpha_o} = 1 - 0.12V_{P_o}$ being V_{α_o,θ_o} the initial volume fractions of ferrite and cementite, respectively, at room temperature. Likewise, $V_{\alpha,\theta,\gamma}$ are the volume fractions of ferrite, cementite and austenite, respectively, at any transformation temperature. The austenite volume fraction was calculated at every temperature using Equations 14 and, 21 or 22. The factors 2 and 1/3 in Equation 24 are due to the fact that, the unit cell of ferrite and cementite contain 2 and 12 iron atoms, respectively, whereas that of austenite has 4 atoms. Moreover, a_{α_o} is the lattice parameter of ferrite at room temperature, taken to be that of pure iron ($a_{\alpha_o} = 2.866$ Å); a_{θ_o}, b_{θ_o}, c_{θ_o} are the lattice parameters of cementite at room temperature [32], given by 4.5246, 5.0885 and 6.7423 Å, respectively; and a_{γ_o} is the lattice parameter of austenite at room temperature as a function of the chemical composition of the austenite [33, 34]:

$$a_{\gamma_o} = 3.573 + 0.033\text{C} + 0.00095\text{Mn} - 0.0002\text{Ni} + 0.0006\text{Cr} + 0.0031\text{Mo} + 0.0018\text{V} \tag{25}$$

where the chemical composition is measured in wt% and a_{γ_o} is in Å.

a_α, a_θ, b_θ, c_θ, and a_γ are the lattice parameter of ferrite (α), cementite (θ) and austenite (γ) at any transformation temperature. They are calculated as follows:

$$a_\alpha = a_{\alpha_o}[1 + \beta_\alpha(T - 300)] \tag{26a}$$

$$a_\gamma = a_{\gamma_o}[1 + \beta_\gamma(T - 300)] \tag{26b}$$

$$a_\theta = a_{\theta_o}[1 + \beta_\theta(T - 300)] \tag{26c}$$

$$b_\theta = b_{\theta_o}[1 + \beta_\theta(T - 300)] \tag{26d}$$

$$c_\theta = c_{\theta_o}[1 + \beta_\theta(T - 300)] \tag{26e}$$

where $\beta_{\alpha,\theta,\gamma}$ are the linear thermal expansion coefficients of ferrite, cementite and austenite, respectively, in K^{-1}. The values of the linear thermal expansion of ferrite and austenite [35] considered in these calculations were $\beta_\alpha = 1.244 \times 10^{-5}$ K^{-1} and $\beta_\gamma = 2.065 \times 10^{-5}$ K^{-1}. Moreover, the thermal expansion coefficient of cementite increases with temperature [32]. Using data published by Stuart and Ridley [32], the expression of the linear expansion coefficient as a function of temperature is:

$$\beta_\theta = 6.0 \times 10^{-6} + 3.0 \times 10^{-9}(T - 273) + 1.0 \times 10^{-11}(T - 273)^2 \tag{27}$$

where T is the temperature in K.

The dilatation curve calculated using Equation 24 for a low-carbon steel with a mixed initial microstructure consisting of ferrite and pearlite under continuous heating conditions (0.05 Ks^{-1} of heating rate) is shown in Fig. 6 in comparison with the corresponding experimental curve. For convenience of discussion, these dilatation curves can be divided in four stages according to the calculated transformation temperatures: (a) from room temperature to the Ac_1 temperature

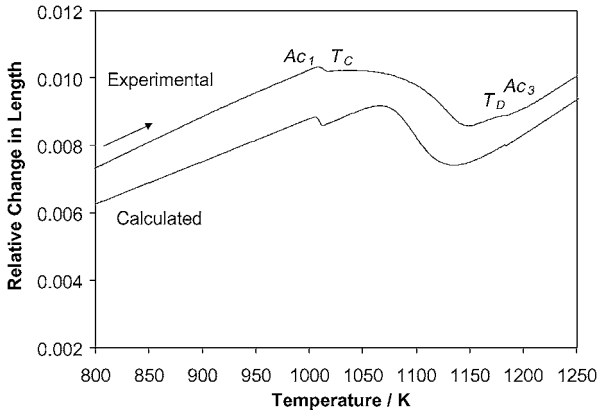

Figure 6 Calculated and experimental dilatation curves of the studied steel for a heating rate of 0.05 Ks^{-1}.

at which pearlite dissolution starts; (b) from Ac_1 to T_C at which pearlite dissolution finishes and ferrite-to-austenite transformation starts; (c) from T_C to Ac_3 temperature at which the transformation of ferrite-to-austenite is finished; and, (d) from Ac_3 to the austenitisation temperature at which non-isothermal heating finishes.

In the first stage, the experimental dilatometric curve exhibits a linear thermal expansion relation with temperature. This is because the initial microstructure of the steel remains unchanged until Ac_1 temperature is reached. In that moment, the relative change in length of the sample no longer follows the linear relation with temperature and it contracts due to the dissolution of pearlite. With increasing temperature and already in the third stage, the relative change in length reach to a maximum, and then decreases until all ferrite is transformed into austenite. This process depends on the competition between the thermal expansion and the ferrite-to-austenite transformation. Thus, even after the relative change in length has reached to a minimum, some ferrite could remain untransformed in the microstructure. This explains the change in the linear thermal expansion as the residual ferrite transforms almost instantaneously at T_D temperature. Beyond that temperature, the sample is fully austenitised, Ac_3 temperature is reached, and the sample exhibits a linear thermal expansion relation with temperature.

In general, the calculated relative change in length was consistent with the measured value at every temperature. The fact that both the modelled and the experimental dilatometric curves run parallel is irrelevant as long as the adequate thermal expansion coefficients are calculated adequately [17]. The linear expansion coefficients [32, 35] of ferrite, cementite and austenite considered in calculations are in a good agreement with those measured values. Experimental kinetic transformation, critical temperatures Ac_1 and Ac_3 as well as the magnitude of the overall contraction due to austenite formation are accurately reproduced by dilatometric calculations. The only difference between both curves corresponds to the general shape of the curve between the onset and the end of the ferrite-to-austenite transformation (i.e., whether or not the specimen continued to get larger for a while after the dissolution of pearlite). That discrepance may be justified by the experimental results of a recent work [36]. This work reported that macroscopic heterogeneous samples with respect to the rolling direction in the steel, very common in hot rolled low carbon steels, undergo an anisotropic dilatation behaviour during transformation of the steel. That possibility is not considered is this model based on isotropic expansion of the sample (see Equation 23).

4. Conclusions

1. Theoretical knowledge regarding the isothermal formation of austenite from pure and mixed initial microstructures has been used to develop a model for the non-isothermal austenite formation in a low-carbon low-manganese steel (0.11C-0.5Mn wt%) with a mixed initial microstructure consisting of ferrite and pearlite. Firstly, a mathematical model applying the Avrami's equation has been used to reproduce the kinetics of the pearlite-to-austenite transformation during continuous heating. The model considers two functions, f_N and f_G, which represent the dependence of nucleation and growth rates, respectively, on the structure. Likewise, Datta *et al*. expressions for the austenitisation kinetics of ferrite-to-austenite transformation at different intercritical annealing temperatures and a mathematical procedure consisting of reiterated differentiation and integration of kinetics functions have allowed to calculate the austenite volume fraction formed from ferrite after pearlite dissolution as a function of temperature for continuous heating conditions.

2. A model of the dilatometric behaviour of the non isothermal pearlite + ferrite-to-austenite transformation has been also developed. The relative change in length which occurs during the austenitisation process has been calculated as a function of temperature. Experimental validation of the kinetics model for the austenite formation has been carried out by comparison between experimental and theoretical heating dilatometric curves. Experimental kinetic transformation, critical temperatures Ac_1 and Ac_3, as well as the magnitude of the overall contraction due to austenite formation are accurately reproduced by dilatometric calculations.

Acknowledgements

The authors acknowledge financial support from Consejería de Educación y Cultura de la Comunidad Autónoma de Madrid (CAM 07N/0065/1998).

References

1. H. K. D. H. BHADESHIA and L. E. SVENSSON, in "Mathematical Modelling of Weld Phenomena" (The Institute of Materials, London, 1993) p. 109.
2. G. A. ROBERTS and R. F. MEHL, *Trans. ASM*. **31** (1943) 613.
3. R. R. JUDD and H. W. PAXTON, *Trans. TMS-AIME* **242** (1968) 206.
4. S. KINOSHITA and R. UEDA, *Trans. Iron Steel Inst. Jpn*. **14** (1974) 411.
5. G. MOLINDER, *Acta Met*. **4** (1956) 565.
6. M. HILLERT, K. NILSSON and L. E. TORNDAHL, *J. Iron and Steel Inst*. **209** (1971) 49.
7. M. NEMOTO, *Met. Trans*. **8A** (1977) 431.
8. G. KRAUSS, in "Steels: Heat Treatment and Processing Principles" (ASM International, Ohio, 1989) p. 274.
9. A. GUSTAVSSON, D. L. McDOWELL, A. MELANDER and M. LARSSON, *Inst. Metallforsk. Forsk. Rapp*. **88** (1994) 3145.

10. V. L. GADGEEL, *Tool Alloy Steels* **28** (1994) 17.
11. C. I. GARCÍA and A. J. DEARDO, *Metall. Trans.* **12A** (1981) 521.
12. G. R. SPEICH, V. A. DEMAREST and R. L. MILLER, *ibid.* **12A** (1981) 1419.
13. M. M. SOUZA, J. R. C. GUIMARAES and K. K. CHAWLA, *ibid.* **13A** (1982) 575.
14. XUE-LING CAI, A. J. GARRAT-REED and W. S. OWEN, *ibid.* **16A** (1985) 543.
15. A. ROOSZ, Z. GACSI and E. G. FUCHS, *Acta Metall.* **31** (1983) 509.
16. J. R. YANG and H. K. D. H. BHADESHIA, *Materials Science and Engineering* A **131** (1991) 99.
17. C. GARCÍA DE ANDRÉS, F. G. CABALLERO, C. CAPDEVILA and H. K. D. H. BHADESHIA, *Scripta Materialia* **39** (1998) 791.
18. F. G. CABALLERO, C. CAPDEVILA and C. GARCÍA DE ANDRÉS, *ibid.* **42** (2000) 1159.
19. L. GAVARD, H. K. D. H. BHADESHIA, D. J. C. MACKAY and S. SUZUKI, *Materials Science and Technology* **12** (1996) 453.
20. C. A. L. BAILER-JONES, H. K. D. H. BHADESHIA and D. J. C. MACKAY, *ibid.* **15** (1999) 287.
21. G. R. SPEICH and A. SZIRMAE, *Trans. TMS-AIME* **245** (1969) 1063.
22. S. F. DIRNFELD, B. M. KOREVAAR and F. VAN'T SPIJKER, *Metall. Trans.* **5** (1974) 1437.
23. D. P. DATTA and A. M. GOKHALE, *ibid.* **12A** (1981) 443.
24. E. NAVARA and R. HARRYSSON, *Scripta Metall.* **18** (1984) 605.
25. E. E. UNDERWOOD, in "Quantitative Stereology" (Addison-Wesley, Reading, 1970) p. 73.
26. S. A. SALTYKOV, in "Stereometric Metallography" (Metallurgizdat, Moscow, 1958) p. 267.
27. R. T. DE HOFF and F. H. RHINES, in "Quantitative Stereology" (McGraw-Hill, New York, 1968) p. 93.
28. M. AVRAMI, *J. Chem. Phys.* **8** (1940) 212.
29. J. W. CHRISTIAN, in "The Theory of Transformations in Metals and Alloys" (Pergamon Press, Oxford, 1975) p. 19.
30. R. G. KAMAT, E. B. HAWBOLT, L. C. BROWN and J. K. BRIMACOMBE, *Metall. Trans.* **23A** (1992) 2469.
31. K. W. ANDREWS, *JISI* **203** (1965) 721.
32. H. STUART and N. RIDLEY, *ibid.* **204** (1966) 711.
33. N. RIDLEY, H. STUART and L. ZWELL, *Trans. of A.I.M.E.* **245** (1969) 1834.
34. D. J. DYSON and B. HOLMES, *JISI* **208** (1970) 469.
35. M. TAKAHASHI, in "Reaustenitization from Bainite in Steels" (University of Cambridge, Cambridge, 1992) p. 91.
36. T. A. KOP, in "A Dilatometric Study of the Austenite/Ferrite Interface Mobility" (Delft University of Technology, Enschede, 2000) p. 30.

Received 11 December 2000
and accepted 26 April 2002